ISSN: 2688-8645

Research on the Remote-Sensing Imaging Characteristics of Ground Penetrating Radar for Leakage from Buried Oil Pipelines in Loess Layers

Teng Wang

School of Pipeline Engineering, Xi'an Shiyou University, Xi'an, Shaanxi, 710000, China

Abstract

When oil contamination occurs in a loess layer, the high porosity of the loess causes rapid signal attenuation. Abnormal dielectric properties produce complex reflected signals, while vertical joints and fissures generate multiple reflections, making it difficult to resolve the details of oil contamination as clearly as in ordinary soils. To clarify the imaging characteristics of leakage from buried oil pipelines in loess, a physical model of buried pipelines under different leakage conditions was established. GprMax was used to simulate multiple leakage scenarios under practical operating conditions. A variety of analysis methods, including neural networks, reflected-wave feature extraction, and imaging-algorithm optimization, were adopted to mine imaging features related to pipeline leakage from the data. The results show that the YOLOv5 neural network has strong feature-extraction capability for forward-simulation images of oil-pipeline leakage and exhibits good generalization in leakage detection.

Keywords

Oil-contaminated Zone; Loess Layer; Ground Penetrating Radar; Imaging Characteristics; Finite-difference Time-Domain.

1. Introduction

Buried oil pipelines are critical infrastructure for energy transportation, and they face many special challenges in loess formations, including the intrinsic properties of loess, fluctuations in groundwater level, and pipeline structural factors. When leakage occurs, timely and accurate detection is essential for safe pipeline operation. Loess itself also has distinctive physical and chemical properties. Its high resistivity, complex dielectric behavior, and other characteristics make conventional leakage-detection methods ineffective or even difficult to apply in loess environments. Compared with other techniques, ground-penetrating-radar (GPR) remote-sensing imaging has certain advantages in detecting subsurface structures and material distribution. However, because of the complexity of loess, its imaging characteristics differ from those in ordinary soils. In-depth study of these special imaging characteristics can improve understanding of the GPR detection mechanism in loess, reduce interference caused by the loess environment, and provide accurate location information for subsequent maintenance such as repair and replacement, thereby avoiding more serious safety incidents caused by undetected leakage.

The hazards caused by leakage from buried oil pipelines have become a research focus in geotechnical engineering and oil-and-gas storage and transportation in recent years, and related studies have been carried out. Gao Feng et al. [1] performed dynamic tensile–compressive mechanical tests on three different rock states to investigate the influence of temperature and water content on the dynamic mechanical properties of rock. Pan Lei et al. [2] studied GPR imaging laws by using the finite-difference time-domain software GprMax to build a highly realistic soil-environment model, simulate electromagnetic-wave propagation in soil

ISSN: 2688-8645

containing voids, and analyze the corresponding radargrams. Zhao Xingyou [3] used GprMax to conduct forward simulations of nonmetallic pipelines under different burial depths and environmental conditions, focusing on how burial depth and environment affect GPR images. Shao Hua [4] first briefly explained the basic principles of three-dimensional GPR and then investigated its practical application in road-crack detection.

Existing studies have made significant progress in the analysis of GPR imaging characteristics for oil-and-gas pipeline leakage. However, the strong attenuation of loess leads to low signal-to-noise ratio and blurred features in GPR images. Traditional manual interpretation depends heavily on experience and is inefficient, so intelligent solutions are needed. Owing to its deep architecture and strong feature-extraction ability, the VGG-16 convolutional neural network has become suitable for complex image analysis. This study proposes combining VGG-16 with GPR imaging to build an automated leakage-recognition framework for extracting and classifying leakage features in loess environments. Xie Huicai et al. [5] trained a BP neural network using radar-waveform parameters as features and showed that it achieved good recognition accuracy for rebar diameter identification. Feng Deshan et al. [6] applied Faster R-CNN and YOLOv3 to the automatic recognition of tunnel GPR images and obtained satisfactory results in recognizing steel arches, reinforcing meshes, and construction joints. Wang Chao [7] applied an improved VGG-16 model to tunnel advanced prediction for automatic recognition of various hazards, and the optimized network achieved both high recognition accuracy and good robustness. Zhang Junhao et al. [8] realized automatic recognition of GPR images by using a convolutional neural network, and their method achieved an identification rate of about 85% for reinforcement and voids in tunnel linings.

Taking oil-and-gas pipeline leakage contamination in loess regions as the research object, this study focuses on GPR imaging characteristics analyzed with neural networks. By combining theoretical analysis with numerical simulation, a leakage model for oil-and-gas pipelines that accounts for the special engineering properties of loess was established. Convolutional neural networks were then used for analysis to reveal the contamination pattern of oil-and-gas pipelines in loess areas, providing a theoretical basis and technical support for the safe operation of such pipelines.

2. Theoretical Basis

2.1. Basic Principles of Ground Penetrating Radar

After an oil pipeline leaks, the released oil diffuses through the loess layer and forms a medium region that differs from the original loess. When the electromagnetic waves emitted by the GPR reach the interface between the oil and the loess, a distinct reflection is produced because of the contrast in dielectric constant. As a result, the radar image shows corresponding anomalous reflection zones, which helps identify the approximate location of the oil leakage. The acquired radar data are then transmitted to a computer and processed using professional radar-data analysis software. Through visualization such as color rendering of depth-profile images, areas with abnormal colors can be observed intuitively, and their shape, position, and relation to the pipeline can be analyzed.

The basic parameters of GPR investigation are described as follows:

Propagation velocity of electromagnetic waves in a medium

$$v = c/\sqrt{\varepsilon_r \mu_r} \approx c/\sqrt{\varepsilon_r} \quad (1)$$

where c is the propagation velocity of electromagnetic waves in vacuum (0.29979 m/ns); εr is the relative dielectric constant of the medium; and μr is the relative magnetic permeability of the medium (generally taken as 1).

ISSN: 2688-8645

During propagation in a medium, when electromagnetic waves encounter a geological interface with an obvious change in relative dielectric constant, reflection and transmission occur. The distribution of reflected and transmitted energy mainly depends on the electromagnetic reflection coefficient of the anomalous interface:

$$r = \frac{(\sqrt{\varepsilon_2\mu_2} - \sqrt{\varepsilon_1\mu_1})^2}{(\sqrt{\varepsilon_2\mu_2} + \sqrt{\varepsilon_1\mu_1})^2} \approx \frac{(\sqrt{\varepsilon_2} - \sqrt{\varepsilon_1})^2}{(\sqrt{\varepsilon_2} + \sqrt{\varepsilon_1})^2} \tag{2}$$

2.2. Introduction to the YOLOv5 Neural Network

YOLOv5 is an advanced object-detection algorithm whose input is typically a 640×640 RGB image. The network uses a CSP (Cross Stage Partial) structure as the backbone, which contains multiple C3 modules and a Focus layer. The Focus layer slices and reorganizes the input image in the spatial dimension to increase the number of channels, while the C3 modules combine residual connections and bottleneck structures to extract image features effectively. Most convolution kernels are 3×3, and feature-map downsampling is achieved through different strides.

In the neck, YOLOv5 uses a PANet structure to realize multi-scale feature fusion through a feature pyramid network (FPN) and a bottom-up path-enhancement strategy, enabling it to handle targets of different sizes.

Detection is performed on feature maps at three different scales to adapt to objects of different sizes.

Finally, YOLOv5 applies non-maximum suppression (NMS) to overlapping bounding boxes and outputs the final detection results. The whole network is concise and efficient and offers fast inference while maintaining high detection accuracy, making it suitable for real-time object-detection scenarios.

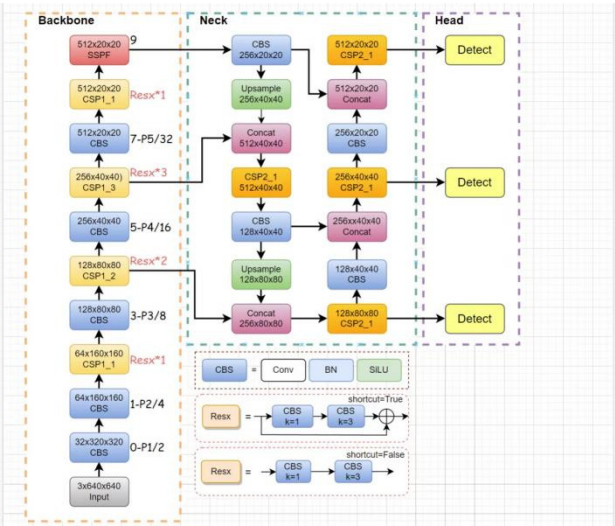

Figure 1. Architecture of the YOLOv5 model

2.3. Dielectric-Constant Characteristics of Loess Layers

The high porosity and vertical joints of loess form a 'honeycomb-like' skeletal structure, which leads to irreversible collapsible deformation when wetted. Unlike sands and ordinary soils, whose mechanical properties are less sensitive to moisture, the mechanical behavior of loess depends strongly on water content. Its collapsibility causes a sharp drop in bearing capacity. In addition, the preferential vertical permeability and joint network of loess can become rapid migration pathways for contaminants.

ISSN: 2688-8645

The main factors affecting the dielectric constant of loess are pore structure, temperature, and frequency. Because loess contains relatively large amounts of air, and because the dielectric constant of air is close to 1 and much lower than that of soil particles and water, a larger porosity generally results in a lower overall dielectric constant. In loess, higher temperature may cause water evaporation, reduce water content, and thus decrease the dielectric constant.

3. Detection of Soil Contamination Caused by Oil-and-Gas Pipeline Leakage Using GPR

3.1. Basic Structural Model of Leakage from a Buried Oil Pipeline in a Loess Layer

The model has a horizontal length of 5.0 m, a detection depth of 3.0 m, a cell size of 0.0025 m × 0.0025 m, and a time window of 60 ns. The relative dielectric constant of loess is 7 and its thickness is 3.0 m. The pipeline is modeled as a PEC pipe with a relative dielectric constant of 4.0 and a thickness of 0.05 m. The dominant frequency of the source wavelet is set to 600 MHz, and a Ricker wavelet is used as the excitation source.

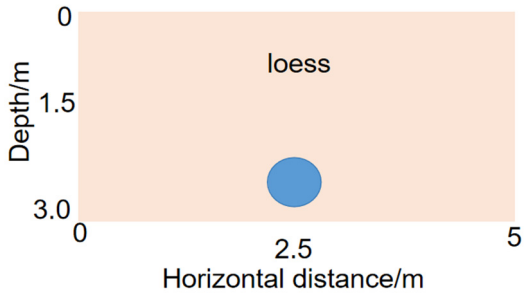

Figure 2. Schematic of GPR modeling

3.2. Basic Pipeline Parameters

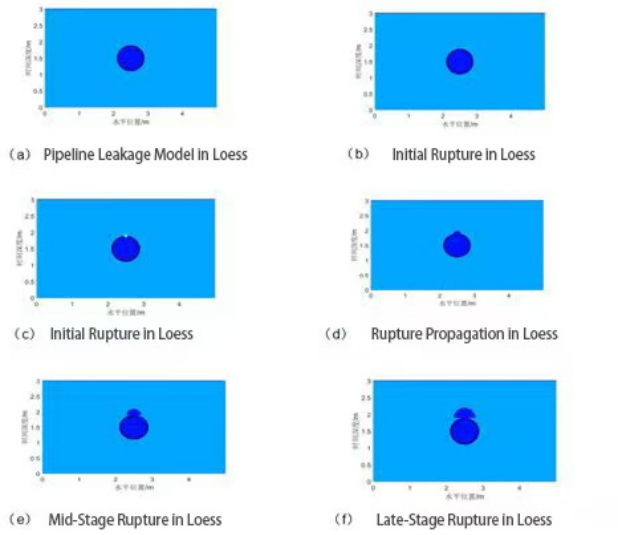

Figure 3. Leakage model of the oil-and-gas pipeline

The buried oil-and-gas pipeline passes through a loess body. The pipeline length in the landslide section is 60 m and the burial depth is 3 m. The pipe material is X80 steel. The main mechanical parameters are as follows: density 8010 kg/m3, diameter 1.612 m, wall thickness 20 mm, total

ISSN: 2688-8645

length 100 m, elastic modulus 210000 MPa, internal pressure 9 MPa, Poisson's ratio 0.3, and yield strength 483 MPa.

3.3. Establishment of the Leakage Model and Forward Simulation for an Oil-and-Gas Pipeline in Loess

Figures a–f represent the model states of an intact pipeline, a ruptured pipeline, the initial rupture stage, and the rupture development stage. The model has a horizontal length of 5.0 m, a detection depth of 3.0 m, a cell size of 0.0025 m × 0.0025 m, and a time window of 60 ns. The relative dielectric constant of the soil is 7 and the thickness is 3.0 m. The pipeline is modeled as a PEC pipe with a relative dielectric constant of 4.0 and a thickness of 0.05 m. The dominant frequency of the source wavelet is set to 600 MHz, and a Ricker wavelet is used as the excitation source. Through 488 trace positions, with 10,177 computational steps for each trace, two-dimensional forward-simulation data were obtained, as shown in Fig. 4:

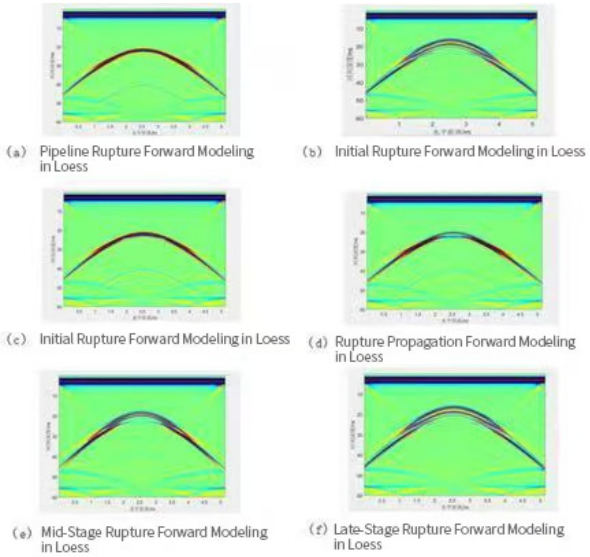

Figure 4. Forward-simulation images of oil-and-gas pipeline leakage

The forward-simulation results [Fig. 3(a)–(f)] clearly show the leakage condition of the pipeline inside the loess. The images have a distinct layered appearance, and the signal characteristics corresponding to different depths and media are clear.

At the same time, the feature analysis of the forward-simulation images indicates that the rupture process of buried oil pipelines in loess exhibits a staged evolution pattern from local initiation to overall expansion. In the initial rupture stage [Fig. b and c], tiny cracks nucleate in local stress-concentration areas. The alternating distribution of low-gray-value regions and high-gradient zones reflects the influence of the heterogeneity of loess on the initial rupture path. During the development stage [Fig. d and f], cracks extend directionally along weak planes in the soil, and the coexistence of banded gray-scale structures and irregular branching reveals the interaction between stratification and shear-failure mechanisms. The intermediate stage [Fig. e] shows a compound mode involving penetration of the main crack and coordinated evolution of a secondary crack network; the enhanced contrast between light and dark indicates the significant response of electromagnetic waves to the reflective properties of rupture interfaces. Through differences in color gradients and texture features, images from each stage intuitively show the spatial distribution of energy release, soil displacement, and

ISSN: 2688-8645

seepage-coupling effects during rupture, providing key visual evidence for evaluating pipeline structural integrity and soil stability.

4. Construction and Testing of the YOLOv5 Model

4.1. Data Preprocessing

Original GPR images containing typical leakage features were obtained through field GPR surveys or public databases, and forward-simulation images (Fig. a–f) were used as supplementary data to simulate leakage patterns under loess conditions. The acquired images were then standardized as follows: the original GPR images were resized to a fixed size of 224×224 pixels to meet the input requirements of the YOLOv5 network; contrast-limited adaptive histogram equalization was applied to enhance the gray-level contrast between cracks and the background while suppressing local overexposure; and Gaussian smoothing with σ = 1.5 was used to remove high-frequency noise caused by the loess medium. A comparison of the images before and after processing is shown in Fig. (a) and (b) (unfinished).

4.2. Dataset Construction

In this study, 200 preprocessed images representing the early, middle, and late stages of oil-pipeline leakage in loess were stored in the images folder. Labelme was then used to annotate the leakage features in the forward-simulation images, and a corresponding label was generated for each image. The completed dataset was then transferred into the file manager in the Anaconda environment for subsequent model training and testing.

4.3. YOLOv5 Model Improvement and Transfer Learning

The model adopted in this paper is based on the YOLOv5s network. After evaluating recognition performance, training speed, and computational speed for radar forward-simulation images of underground oil-pipeline leakage, YOLOv5s was finally selected as the detection model. Since the input data are three-channel RGB radar forward-simulation images, the original three-channel input was retained to match the standard YOLOv5 input format (640×640×3), avoiding information loss caused by channel conversion and preserving the electromagnetic-response differences between the leakage zone and the surrounding medium.

In the backbone design, the CSPDarknet structure of YOLOv5 is retained, but the initial number of channels in the first two convolutional layers is adjusted to enhance the extraction of low-frequency electromagnetic features in radar images. For the special target morphology in underground oil-pipeline leakage scenarios—such as elongated pipeline bodies and irregular leakage-diffusion areas—the weight allocation for medium-scale features larger than 32×32 pixels is increased in the PANet-based neck. Cross-stage partial connections are used to strengthen semantic association across features at different depths, thereby effectively distinguishing the strong reflection of the metallic pipeline body from the weak scattering signal of the leakage-diffusion area.

4.4. Model Training and Testing

Automatic recognition using neural networks usually requires tens of thousands of samples to obtain stable generalization ability. However, the YOLOv5s model used in this study still showed excellent performance under a small-sample condition. Considering the high cost of radar forward simulation for underground oil pipelines, only a dataset containing 200 samples was prepared in this study. Repeated debugging showed that the best effect was achieved when the number of iterations reached 100; the loss value then approached zero, indicating that the model reached an optimal solution. The overall loss curve of the model is shown in Fig. 5.

ISSN: 2688-8645

5. Image Recognition Analysis

After the model was trained and tested, it could automatically recognize any preprocessed radar forward-simulation image of a buried oil pipeline. To verify the accuracy of this automatic recognition, nine radar forward-simulation images of leaked oil pipelines were randomly selected for testing, as shown in Fig. 6.

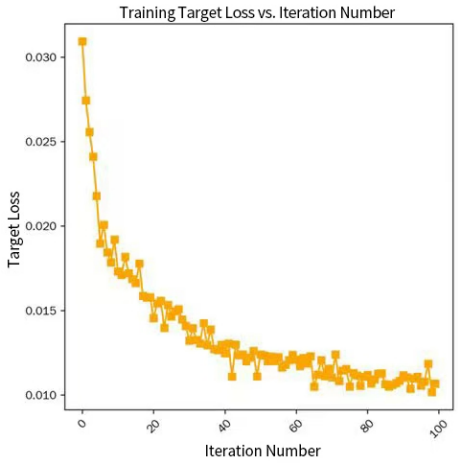

Figure 5. Overall loss curve of the YOLOv5 model

The test results show that, on the constructed GPR forward-simulation test set, the model achieved a recall of 99% for leakage samples, effectively verifying its accurate discrimination of leakage features. Meanwhile, for non-leakage GPR forward-simulation images in the test set, the model achieved a false-alarm rate of 0. These experimental results fully demonstrate that, through deep-network learning, the model has built highly discriminative feature representations for leakage and non-leakage scenarios, showing strong generalization ability and providing core theoretical support for engineering application of the method.

6. Conclusion

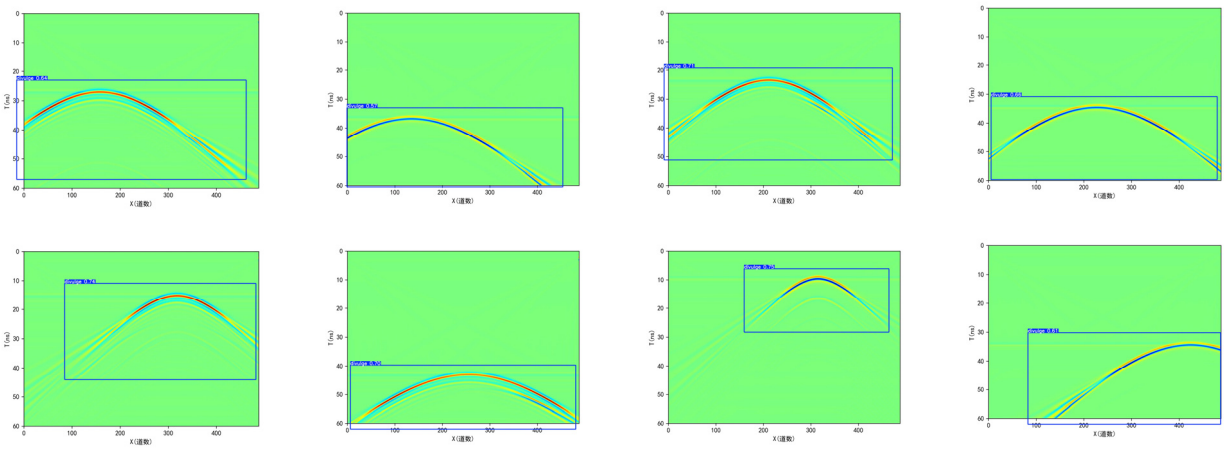

Figure 6. Prediction results for leaking pipelines

(1) The detection model built on the YOLOv5 framework successfully realized automated detection of radar forward-simulation images of underground oil-pipeline leakage, effectively

identifying leaked buried oil pipelines and providing an intelligent solution for pipeline safety monitoring.

(2) By optimizing backbone feature extraction, adjusting the neck multi-scale feature-fusion strategy, and adaptively designing the anchor-box parameters in the detection head, the model achieved precise capture of leakage features even with a small dataset of only 200 radar forward-simulation samples, meeting the real-time detection requirements of edge devices.

(3) Under complex geological conditions, where radar echo interference is strong and the boundary between the leakage zone and the pipeline body is blurred, the detection accuracy for micro-leakage (oil-phase proportion < 5%) still has room for improvement. In future work, transfer learning and attention mechanisms can be incorporated to further improve recognition of weak-signal features.

References

[1] Gao Feng, Yang Gen, Xiong Xin, et al. Experimental study on the dynamic mechanical properties of slope rock under low-temperature conditions [J]. Journal of Engineering Science, 2023, 45(2): 171-181.

[2] Pan Lei, Wan Xinlin, Sun Tianyu, et al. Forward simulation and study of underground cavities by ground penetrating radar based on GprMax [J]. Anhui Architecture, 2021, 28(11): 167-169.

[3] Zhao Xingyou. Application of ground penetrating radar in the detection of nonmetallic pipelines [J]. Jiangxi Building Materials, 2021(12): 130-132.

[4] Shao Hua. Application of three-dimensional ground penetrating radar in road-crack detection [J]. Engineering Construction and Design, 2022(02): 73-75.

[5] Xie Huicai, Xu Maohui. BP neural-network recognition of reinforced-concrete radar signals [J]. Journal of Huazhong University of Science and Technology (Urban Science Edition), 2007, 24(1): 1-4, 12.

[6] Feng Deshan, Yang Zilong. Automatic recognition of tunnel-lining structural GPR images based on deep learning [J]. Progress in Geophysics, 2020, 35(4): 1552-1556.

[7] Wang Chao. Research and application of an optimized convolutional neural-network model for classification of measured tunnel GPR data [D]. Xi'an: Chang'an University, 2019.

[8] Zhang Junhao, Zhao Junfeng, Liu Liyuan. Tunnel lining detection by ground penetrating radar based on convolutional neural networks [A]// Proceedings of the 2021 Academic Exchange Conference on Industrial Buildings [C]. 2021: 576-579.